Articles

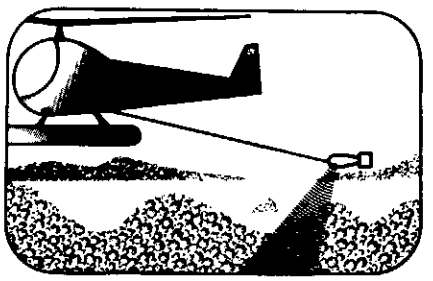

Remote Sensing in Mineral Exploration - Case Histories

J.A.E. Allum
Inco Metals Company
Box 44, 1 First Canadian Place
Toronto, Ontario M5X 1C4

Summary
Situations are discussed in which remote sensing has helped in the exploration for silver, fluorite, gold, bauxite, ilmenite, and nickel. It is shown that remote sensing can be a specific tool, in tropical rain-forest terrains, for the exploration for nickel-laterite deposits. It is also shown that the combined use of an airborne gamma-ray survey with the interpretation of a satellite image is an effective method of exploring for heavy-mineral sands.

Introduction
This paper is an enlarged version of a talk given to the Prospectors and Developers Association Annual Convention in March 1979. It describes a number of case histories in which remote sensing assisted in mineral exploration. The cases are a selection from those in which the author was personally involved. No attempt has been made to discuss all remote sensing methods and their application to mineral exploration.

The types of remote sensing referred to in this paper are aerial photography, satellite imagery, and synthetic aperture radar (SAR) imagery. For readers who are unfamiliar with remote sensors and their application, the following references are given: for aerial photographs, Allum (1966); Miller (1961); Ray (1960); for radar imagery, Mekel (1972); for Landsat imagery, Anon., (1976); Rowan *et al.*, (1974); Viljoen *et al.*, (1975); and for remote sensing in general, Sabins (1978) and Verstappen (1977).

Under appropriate conditions remote sensing can be used: (1) as a tool for finding certain surface mineral deposits; (2) to find extensions to known mineral deposits; (3) to find new mineral deposits in the same geological environment and the same general area as known deposits; (4) as an exploration method to be integrated with other methods such as geophysics and geochemistry in an exploration program; (5) as a method of selecting geologically favourable areas for particular types of deposits, when planning an exploration program.

Some surface deposits such as iron ore, bauxite, and nickel laterite, in tropical rain-forest terrain, can be interpreted directly on aerial photographs with a fair degree of confidence. Such interpretation, which is an example of the first use listed above, has been done with particular success in the Amazon Basin.

A photogeologist cannot make an indubitable interpretation that a particular area is covered by bauxite or nickel-laterite. What he can do is to point out particular areas as targets for nickel-laterite or bauxite exploration. He does not interpret nickel-laterite as such; he interprets an ultramafic rock body in a tropical rain-forest environment, and proposes it as a target for nickel-laterite exploration. (It is well known that ultramafic rocks, suffering tropical rain-forest weathering for a prolonged period, develop a capping of nickel-laterite.)

Similarly, if the photogeologist interpreted an area of residual superficial cover lying on limestone in a tropical rain-forest environment, he would propose the area as a target for bauxite exploration. His justification for this would be his knowledge, gained from the literature, of bauxite deposits elsewhere (e.g., Jamaica, Rennell Island).

Once the remote sensing interpreter has achieved success with a particular type of deposit in a particular geological and erosional environment, he may be able to find similar deposits in the same general area. This is because he then knows exactly what he is looking for.

The case histories that follow exemplify some of the above comments.

Amazon Basin, Brazil (BIF)
In tropical rain-forest areas, where enough erosion is taking place to produce differential relief, it is possible to discriminate between ortho-quartzite and siliceous banded iron formation (BIF) on both aerial photographs and synthetic-aperture radar (SAR) imagery. This ability is of importance in mineral exploration, because it assists in the correct interpretation of bedded volcanic rocks that are possible hosts of volcanogenic massive sulphide deposits. The interpreter assumes that there is a good possibility that the conformable, bedded, sedimentary-looking rocks associated with the BIF are in fact volcanics. He therefore selects them as targets to be field-checked for volcanogenic massive sulphide deposits. The criteria for discriminating by remote sensing between ortho-quartzite and BIF will be suggested by the following considerations.

Sand is typically deposited over a large area in sequential association with muddy sand and mud. After isoclinal folding and metamorphism, the resulting steeply dipping ortho-quartzite normally forms a sharp ridge associated with more subdued, parallel ridges of metasediments. Because of the large original area of deposition, the isoclinal folding may result in the whole set of parallel ridges being repeated several times.

Banded iron formation and the associated volcanics formed by submarine volcanic (exhalative) processes are, however, typically deposited over a considerably smaller area than the sediments discussed above. After folding, the now steeply dipping BIF would be likely to form a sharp ridge very similar in photographic appearance to that of the ortho-

0315-0941/81/03/087-092 $01.00/0

quartzite. Because of the more limited original areal extent of the BIF and associated volcanics, however, they may show little or no repetition after isoclinal folding.

A related criterion for discriminating between ortho-quartzites and BIF is that of the lengths of the ridges formed by them after metamorphism and isoclinal folding. Ortho-quartzite ridges can be of any length, but the lengths of the BIF ridges are limited to the maximum volcanogenic dimension of the original area over which the BIF was deposited.

Thus isolated sharp ridges of moderate length would be interpreted as probably representing BIF, whereas long, sharp ridges, exhibiting more repetition by folding, would be interpreted as probably representing ortho-quartzite.

The ridge at the NE corner of the aerial photograph in Figure 1 (point 4) represents banded iron formation, which can be seen again in the SAR image Figure 2, (point 2). The solitary nature of the ridge (point 2) on Figure 2, and its limited extent along strike (not visible on Figures 1 and 2), provide criteria that should enable the volcanogenic BIF to be correctly interpreted. This interpretation should in turn enable the rocks at the west end of the banded iron formation (Figure 2, point 3) to be correctly interpreted as volcanics. They are in fact volcanics associated with lead and zinc sulphide mineralization (Robin Ball, pers. commun.).

These remote sensing criteria (solitary nature of ridge, and limited extent along strike) have enabled many other volcanogenic banded iron formations to be interpreted in the area.

Amazon Basin, Brazil (Nickel-Laterite)

The exploration for nickel-laterite in a tropical rain-forest terrain consists essentially of looking for large, ultramafic rock bodies, in the expectation that, if they have been exposed to weathering for a sufficient length of time, they will be covered by the required deposit.

The diagnostic characteristics that enable large bodies of ultramatic rocks, in a tropical rain-forest environment, to be interpreted are: (1) rounded topography, (2) absence of jointing visible at the scale of the photograph, (3) uniformity of vegetation cover in comparison with that of the surrounding rocks. The uniformity of vegetation cover results in a velvety appearance on aerial photographs. It is the most reliable of the above criteria. The cause of this vegetation cover uniformity is probably the paucity of phosphorous and potassium in ultramafic rocks. Very few species of vegetation can thrive in the absence of these elements.

On Figure 1, the rock body at point 1 was interpreted photogeologically as possibly representing an ultramafic rock, and thus being a promising exploration target for nickel-laterite. (Field work confirmed that the rock body was a serpentinite covered by nickel-laterite.) The massiveness, rounded topography absence of jointing visible at the scale of the photography, and the uniformity of vegetation cover in comparison with that of the surrounding granitic basement (compare point 1 with point 3) are diagnostic characteristics.

At point 2 in Figure 1 there is no vegetation; this probably results from metal ions poisoning all vegetation.

An extension to the ultramafic body on Figure 1 (point 1) is represented on the SAR image (Figure 2) by the rock body at point 1. In the NE corner of Figure 2 there is a rock body (point 4) that is somewhat similar to that at point 1 on the same figure. An enlargement of the SAR image of the eastern extension of this second body is shown in Figure 3.

Comparison of the SAR image Figure 3 (near point 1) with the aerial photograph Figure 1 (near point 1) leaves little doubt that the rock body on Figure 3 is of the same kind as that on Figure 1.

Aerial photographs of the area covered by Figure 3 were obtained, after the rock body on Figure 3 had been interpreted on the SAR imagery as being similar to the ultramafic body on Figure 1. Part of one of these aerial photographs is depicted in Figure 4. Comparison of the rock body on Figure 4 with the rock body (1) on Figure 1 leaves no doubt that the two rock bodies are of the same type. The rock body on Figure 4 shows the same massiveness, rounded topography, absence of jointing visible at the scale of the photograph, and uniformity of vegetation; it also shows the same occasional bare patches (see white patches NW of point 2 on Figure 4 and at point 2 on Figure 1).

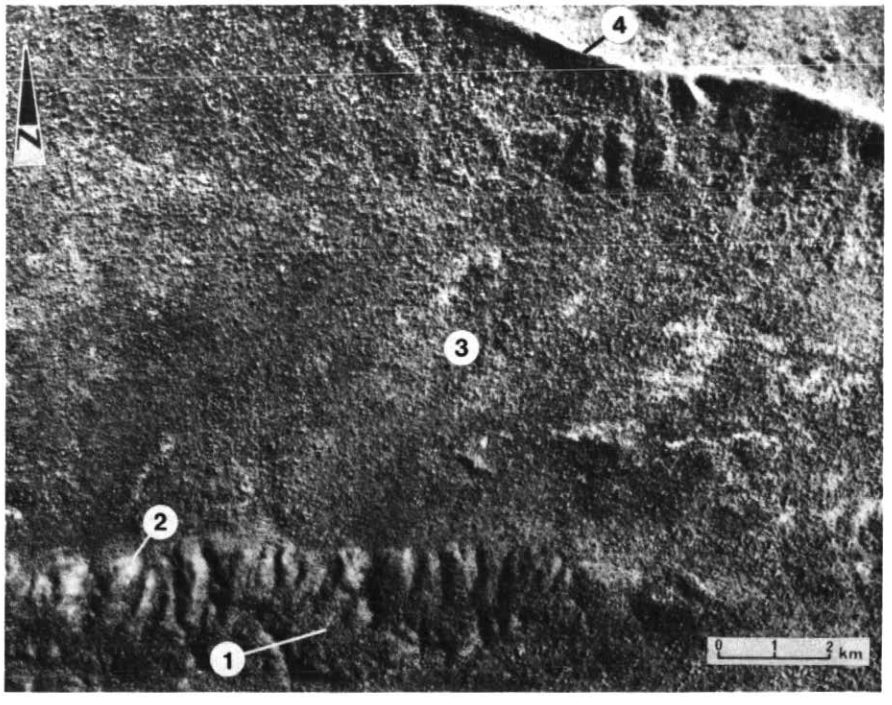

Figure 1 *Aerial photograph showing nickel-laterite covered serpentinized peridotite (1), and banded iron formation (4), in the Amazon Basin, Para State, Brazil.*

Figure 2 *Radar image showing nickel-laterite covered serpentinized peridotite (1) and (4), banded iron formation (2), and volcanics (3) in the Amazon Basin, Para State, Brazil.*

Thus the interpretation of aerial photograph (Figure 1) led to the discovery of the first nickel-laterite deposit overlying ultramafic body (1), which is represented on the SAR image Figure 2 (point 1). Then the general resemblance of a second rock body (4) with the first rock body (1) on Figure 2, resulted in the second rock body being selected as a target for nickel-laterite exploration, and for aerial photographs being obtained for it. Finally field work confirmed that the second body is also a nickel-laterite covered serpentinite.

The SAR image Figure 3, and the aerial photograph Figure 4 (both of the second ultramafic body) have been annotated with the same points, so that the reader can compare the different representations (SAR imagery and aerial photography) of the same places on the ground. The appearances of the rock body on the two types of images are very similar.

A third body of ultramafic rock, some 70 km west of the areas shown in Figures 3 and 4, was interpreted on aerial photographs (see Figure 5). The enlarged SAR image of this third body is shown in Figure 6. The rounded, and general massive appearance on the radar imagery makes the discrimination of the ultramafic rock from the surrounding rocks fairly reliable. This rock body also proved to be a serpentinite covered with nickel-laterite.

The annotated points on aerial photograph Figure 5 correspond to the same numbered points on the SAR image Figure 6. If the two figures are compared, it will be noted that the faults and characteristic rounded topography of the serpentinite show more clearly on the SAR image than on the aerial photograph. It should be remembered, however, that aerial photographs are normally viewed stereoscopically, under which conditions the rounded topography and faults are obvious.

Because SAR imagery is usually viewed non-stereoscopically, it is less time-consuming to use than aerial photographs. SAR imagery, however, does not show the texture of vegetation, which is an important criterion for the interpretation of ultramafic rocks. The selection of nickel-laterite targets in tropical rainforest environments can therefore be carried out more quickly on SAR imagery, but the reliability of the work is greater on aerial photography.

Brunswick Area, U.S.A. (Heavy Mineral Sands)

In 1975 there was a request to carry out a reconnaissance for leucoxene-bearing, heavy-mineral sands, in the south-east

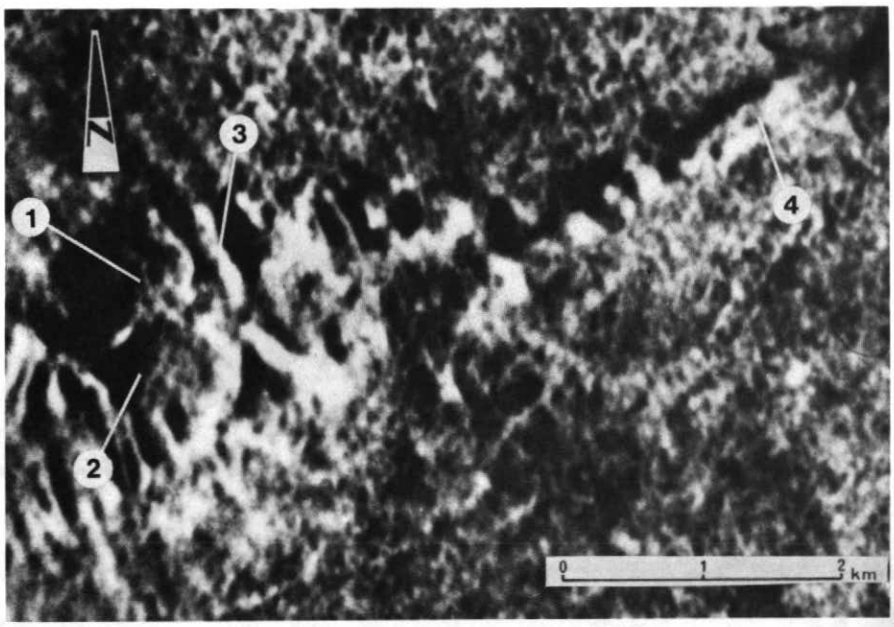

Figure 3 *Enlarged radar image of nickel-laterite covered serpentinized peridotite (1) in the Amazon Basin, Para State, Brazil.*

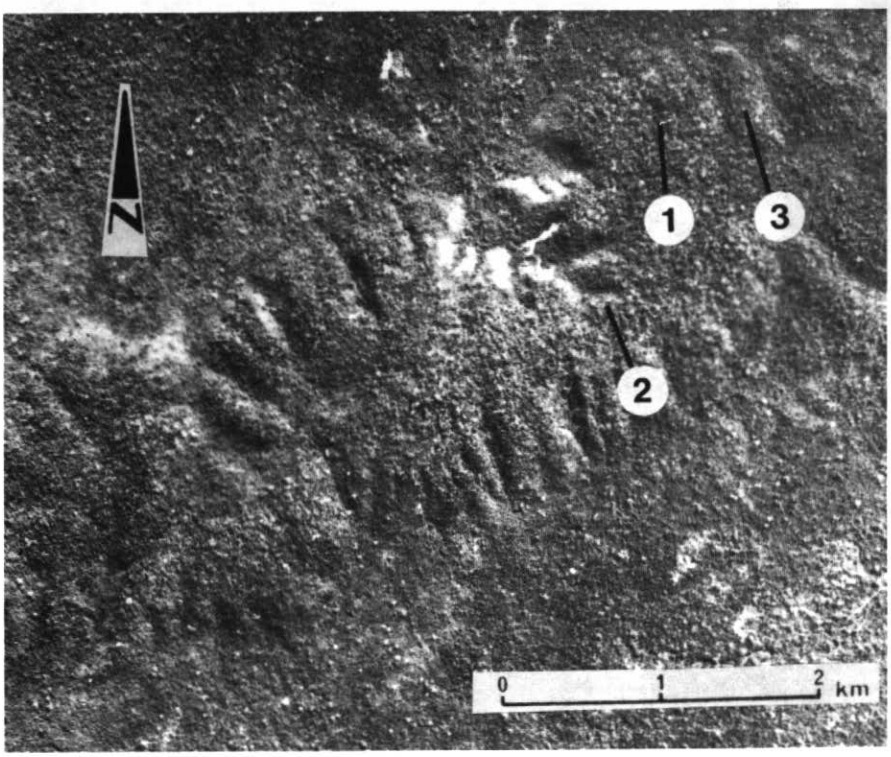

Figure 4 *Aerial photograph of nickel-laterite covered serpentinized peridotite (same body as Figure 3).*

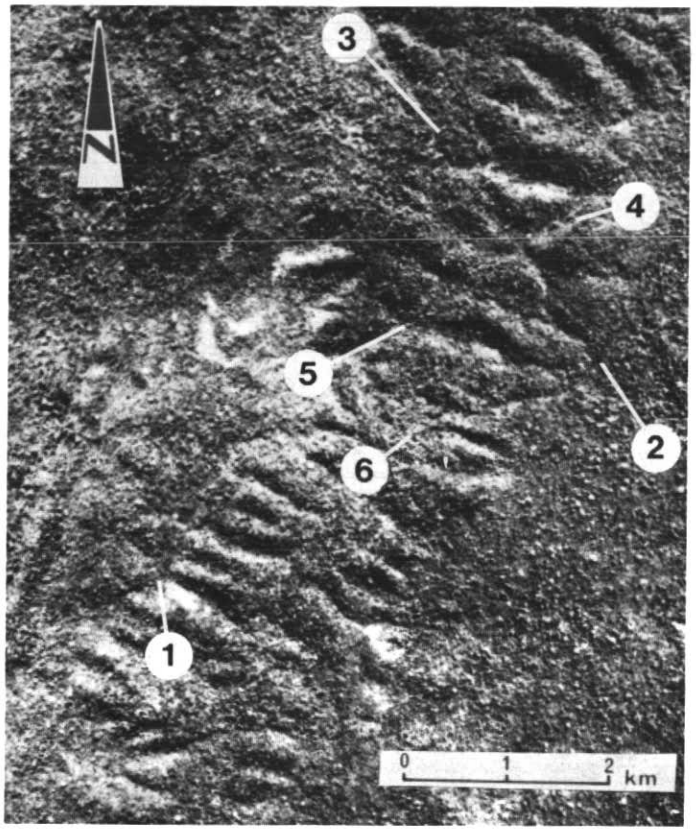

Figure 5 *Aerial photograph of nickel-laterite covered serpentinized peridotite, in the Amazon Basin, Para State, Brazil.*

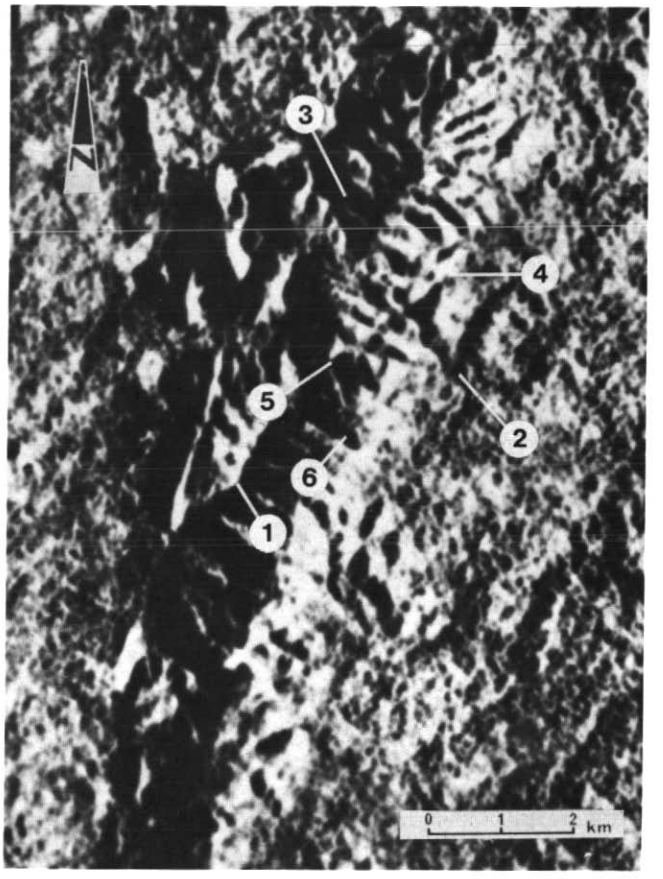

Figure 6 *Enlarged radar image of nickel-laterite covered serpentinized peridotite. Same body as Figure 5.*

U.S.A. Fortunately, a Department of the Interior, Open File Report (Anon. 1975) had recently become available. This report gave details of an airborne radioactivity (gamma-ray) survey of parts of the SE Coastal Plain U.S.A.; it included 15 maps depicting in contour fashion the total radioactivity of the regions flown. The line spacing of the aerial survey was one mile, and the flying height 500 ft.

When ilmenite is weathered, it is gradually altered into the more valuable mineral leucoxene. Thus the older the beach sands are, the richer they are likely to be in leucoxene. The older beach sands are therefore the targets for exploration. Ilmenite is associated with monazite and zircon in the heavy-mineral sands of this area. As these latter minerals are radioactive, they give rise to gramma-ray anomalies.

Unfortunately many gamma-ray anomalies occur over areas that are not sands. Anomalies are common over river alluvium, swamps, granite outcrops, towns, and so on. If therefore it were possible to confine the field checking of gamma-ray anomalies to those areas underlain by ancient beach sands, exploration for leucoxene-bearing heavy-mineral sands would be more cost-effective.

A small portion of a satellite image (Landsat image, E-1279-15280, Band 5) of an area around Savannah, Georgia, is given in Figure 7. Modern beach strand lines are depicted at points 1, 2, and 3; and older beach strand lines are depicted at points 4, 5, and 6 further from the coast. (Agricultural activity has emphasized the old strand lines.) Figure 7 demonstrates that remote sensing, using satellite imagery, can assist in the exploration for leucoxene-bearing heavy-mineral sands by: (1) showing the distribution of the sands, (2) discriminating between the older and younger sands, (3) avoiding the waste of time and money field-checking gamma-ray anomalies lying over areas that are not sands (i.e., alluvium, swamps, granite outcrops, etc.).

A comparison of the satellite imagery with the results of an airborne gamma-ray survey brought to our notice heavy-mineral sand deposits of economic size and grade just south of the area shown in Figure 7. The deposits were, however, already known locally, and by the Georgia Department of Natural Resources.

Rennell Island, Solomon Islands (Bauxite)

In 1966 when an aerial geophysical survey of the then British Solomon Islands Protectorate was carried out by the United Nations, one of the smaller islands (Rennell) was found to have a gamma-ray anomaly near its centre. Since all coral reefs in the area produced gamma-ray anomalies, this in itself, did not justify much interest. When, however, a photo-geological interpretation of Rennell Island was superimposed on the gamma-ray results, it was seen that the major gamma-ray anomaly lay not over the coral, but over sedimentary rocks that were recorded on the interpretation as being lagoonal deposits (Allum 1967).

The association of the gamma-ray anomaly with the sediments rather than with the coral, indicated that the sediments should be sampled and analyzed. These samples were reported by Mineral Resources Division, Overseas Geological Surveys (U.K.), to consist of silica-free bauxite (Allum, 1967, p. 70).

The Rennell bauxite deposit subsequently proved to be of economic size and grade.

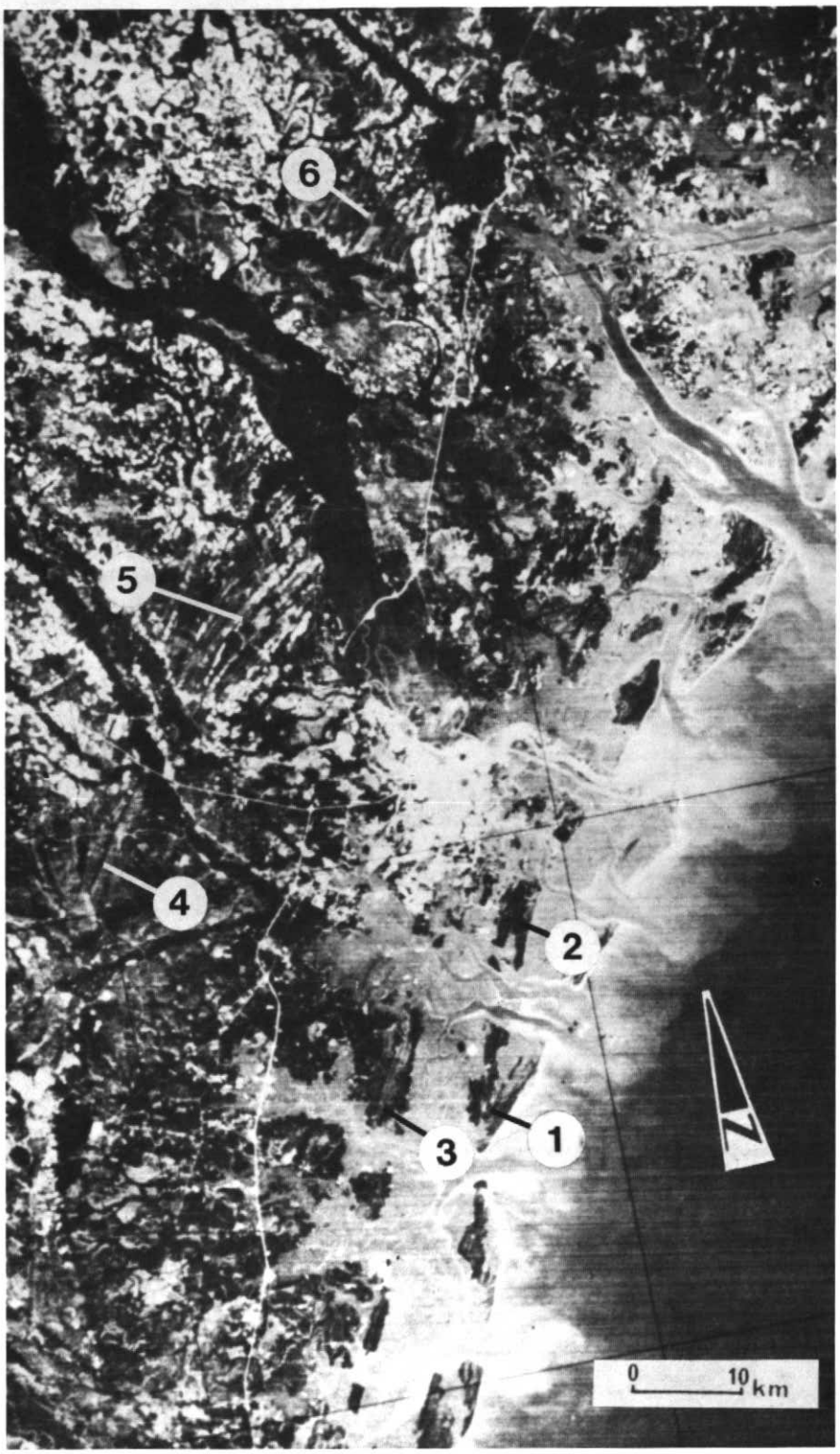

Figure 7 *Satellite image showing recent and ancient beach strand lines in vicinity of Savannah, Georgia, south-east U.S.A.*

Geita Area, Tanzania (Gold)

In 1961, a photogeological interpretation of an area near the Geita Gold Mine was made. The area had already been surveyed by airborne magnetic and electromagnetic methods. When the photogeological interpretation, which had been made without reference to the geophysical results, was super-imposed on the mapped geophysical results, all the geophysical anomalies, except one, could be related to features on the interpretation. The geophysicists then requested that another effort be made to determine the cause of the unexplained anomaly. On looking again at the photographs of the area, a previously unnoticed hair-line lineament was interpreted. The aerial photographs gave no indication of the cause of the lineament, but it was possible on the photographs to indicate its location precisely. This enabled a field crew to determine the cause of the anomaly with one short trench. Field checking showed that the lineament, in fact, represented a non-economic sulphide vein.

This experience showed that remote sensing can indicate some of the causes of geophysical anomalies and thus remove the necessity of field-checking them. This, in itself, produces a considerably saving in time and money spent on field work. It also showed that geophysics can draw attention to features on aerial photographs that are beneath the normal threshold of interpretability for the photogeologist. When the photogeologist is told that there is something there, he may then be able to see it, and determine exactly where it is. This precise location of the cause of the geophysical anomalies considerably reduces the amount of trenching or drilling necessary to test them.

Guanajuato Area, Mexico (Silver), Zaragoza Area, Mexico (Fluorite)

Where the geological environment of a particular type of sub-surface ore deposit is well known, an interpreter may be able to select exploration targets entirely on the evidence of remotely sensed data. One example of this situation is that of the silver veins near Guanajuato. In order to find exploration targets in this area, all the interpreter had to do was to study the relevant aerial photographs stereoscopically, and interpret fracture lineaments that were in close proximity to known mineralized veins. These fracture lineaments represented the targets for further exploration.

The Zaragoza Area, is another example. Here there are major fluorite deposits in limestone, near an unconformity between limestone and overlying volcanics. These deposits are located at either

end of a long lineament, which is expressed only intermittently in the area of volcanics. It was assumed in this case that this lineament was the surface expression of a major fault that provided a path for the mineralizing solutions. The procedure therefore for the successful selection of exploration targets for fluorite was: (1) to interpret photogeologically the unconformity between the limestone and the volcanics; and (2) to find photogeologically, faults that apparently cut both the unconformity and the long lineament. The places where the faults (2) cut the unconformity (1) were selected as the exploration targets. The initial investigation of these targets led to the discovery of mineralized areas which were worth staking.

Discussion

As may be surmised from the case histories given above, there is no single routine by which remote sensing may be cost-effectively utilized in mineral exploration. Each exploration project presents a different problem. The recommended approach is for each exploration project to be considered by a remote sensing interpreter, who is well versed in economic geology.

Knowledge of economic geology is necessary, because the remote sensing interpreter has to decide: (1) what data are relevant to the exploration project; (2) which of the data in (1) can in principle be obtained by remote sensing methods; and (3) which methods to use to obtain the data referred to under (2). Also, the interpreter needs to be able to assess the significance, in terms of economic geology, of the data he obtains; in particular, he needs to be able to recognize the economic significance of unexpected data.

The interpreter should have considerable practical experience in photogeology (i.e., the interpretation of stereo-pairs of aerial photographs), because aerial photography is by far the most used remote sensing method.

Much remote sensing work has ultimately to be collated with the data from geochemistry, geophysics, and geological field work. Because of the usually small scale and the absence of detailed drainage, the results obtained from the interpretation of satellite or SAR imagery, are more difficult to collate with these other data than is a photogeological interpretation, which is at a relatively large scale and which includes detailed drainage.

Acknowledgements

I wish to express my thanks to: Dr. Acyr Avila de Luz (Director General do DNPM and Presidente to Projector RADAM-BRASIL) for permission to publish aerial photographs Figures 1, 4, and 5, and radar images Figures 2, 3, and 6; NASA for supplying Figure 7 and for their help and advice over the years; Merrill Weale for printing the photographs; R.A. Johnson and D. McEachern for mounting and annotating the photographs; Inco Metals Company for permission to publish this paper. The Brazilian field information was all supplied by R. Ball.

References

Allum, J.A.E., 1966, Photogeology and Regional Mapping: Pergamon Press Ltd.

Allum, J.A.E., 1967, Regional photogeological interpretation of the British Solomon Islands: Aerial Geophysical Surveys Project (UNSF-BSIP) 1965-1968.

Anon., 1975, Open file report No. 75-400: Department of the Interior, U.S.A.

Anon., 1976, Landsat Data Users Handbook: Document No. 76SDS4258, NASA, Goddard Space Flight Center, Maryland, 20771, U.S.A.

Mekel, J.F.M., 1972, The Geological Interpretation of Radar Images: ITC Text Book of Photo-Interpretation, Volume VIII, 2, International Institute for Aerial Survey and Earth Sciences (ITC), Enschede, The Netherlands.

Miller, V.C., 1961, Photogeology: McGraw-Hill Book Company, Inc.

Ray, R.G., 1960, Aerial photographs in geologic interpretation and mapping: United States Geological Survey, Professional Paper 373.

Rowan, L.C. *et al.*, 1974, Discrimination of rock types and detection of hydrothermally altered areas in south-central Nevada by the use of computer enhanced ERTS images: United States Geological Survey, Professional Paper 883.

Sabins, F. F. Jr., 1978, Remote Sensing, Principles and Interpretation: San Francisco, W.H. Freeman and Company.

Verstappen, H. Th., 1977, Remote Sensing in Geomorphology: Elsevier Scientific Publishing Company.

Viljoen, R.P. *et al.*, 1975, ERTS-1 imagery: an appraisal of applications in geology and mineral exploration: Minerals Science Engineering, v. 7, no. 2, April, p. 132-167.

MS received January 21, 1981;
Revised March 9, 1981